Reductive Quenching of the Emission of *trans*-Dioxo(1,4,8,11-tetramethyl-1,4,8,11-tetraazacyclotetradecane)osmium(VI) in Water

Siegfried Schindler, Edward W. Castner, Jr., Carol Creutz,* and Norman Sutin

Chemistry Department, Brookhaven National Laboratory, Upton, New York 11973

*Received March 31, 1993**

Reductive quenching of the red emission of the metal-centered excited state of the title osmium(VI) complex (0.3 mM, lifetime 1.0 μs) has been characterized in water at 25 °C (0.5 M ionic strength). The excited state is a very strong oxidant and is very rapidly quenched by a number of moderately reducing anions (anion, $10^{-9}k_q$, M^{-1} s^{-1}): NO_2^-, 2.0; N_3^-, 4.0; I^-, 6.5. The rate constants for quenching by aqua ions are in fair agreement with values calculated from the Marcus cross-relation and self-exchange rates for the $*Os^{VI}(tmc)O_2^{2+}/Os^{V}(tmc)O_2^{+}$ couple (k_{ex} = 1 × 10⁵ M^{-1} s^{-1}) and the aqua ion couple (aqua ion, k_q): $Fe(H_2O)_6^{2+}$, 1.0 × 10⁹ M^{-1} s^{-1}; $Co(H_2O)_6^{2+}$, 1.0 × 10⁶ M^{-1} s^{-1}; $Ce^{III}(aq)$, ≤1.0 × 10⁵ M^{-1} s^{-1}. The k_q (M^{-1} s^{-1}) values for quencher (Q) = Cl^- (4 × 10⁵), HCO_2^- (1.5 × 10⁶), Br^- (1.7 × 10⁸), SCN^- (5.6 × 10⁹), CO_3^{2-} (1.6 × 10⁸), and OH^- (1.0 × 10⁷) are used to estimate self-exchange rate constants for the Q^+/Q couples. The first estimates are presented for the CO_3^{2-}/CO_3^- (0.4 M^{-1} s^{-1}), OH^*/OH^- (300 M^{-1} s^{-1}), and HCO_2/HCO_2^- (300 M^{-1} s^{-1}) couples. Self-exchange rates for the X^*/X^- halogen couples, calculated assuming that only the outer-shell barrier contributes to the intrinsic barrier to outer-sphere electron transfer and that a two-sphere dielectric continuum model is applicable, are orders of magnitude smaller than the self-exchange rates inferred from the quenching data and literature data.

Introduction

The excited states of transition-metal complexes can be powerful reductants and oxidants, depending on their ground-state redox properties and their excitation energies. While the metal-to-ligand excited states characterized to date may be regarded as only moderately strong oxidants, with excited-state reduction potentials in the +1 V vs NHE range,[1-3] some ligand-centered and metal-centered excited states are significantly stronger oxidants. Thus the metal-centered excited state $*Cr(bpy)_3^{3+}$, with an excited-state reduction potential ($*E°$) of +1.44 V, and the ligand-centered excited state $*Ir(Me_2phen)_2Cl_2^+$, with $*E°$ = +1.38 V,[4] are very rapidly reduced by a number of reductants. Recently, a new class of excited-state oxidants ($*E° \sim +1.4$ V) based on ligand-to-metal excited states of Ta(V) was described.[5] While not transition-metal-based species, excited states of $U^{VI}O_2$ are exceptionally strong oxidants ($*E° \sim 2.6$ V vs NHE)[6] which have recently been used to estimate redox potentials of ≥2.0 eV for organic carboxylates. Recently described oxomolybdenum(V) (d^1) species[7] are also likely to be of this class. In view of the small number of strongly oxidizing, emissive excited states of metal complexes, the report of a new class of such species, dioxoosmium(VI) complexes,[8] was of considerable interest. In these complexes, the equatorial sites surrounding the trans dioxo moiety are occupied by cyanide ligands or a tetraaza macrocycle.

The macrocyclic dioxoosmium(VI) complexes are obtained from the oxidation of the corresponding osmium(III) macrocycles and exhibit an intense $\nu(OsO_2)$ stretch at 870 cm^{-1} in the infrared spectrum. From the work of Winkler and Gray[9] on isoelectronic Re(V) systems, the Os(VI) species are discussed in terms of the following molecular orbital diagram (the M–O bond is the z axis and the equatorial ligands lie on the x and y axes):

The d^2 dioxoosmium(VI) has a diamagnetic $^1A_{1g}[(b_{2g})^2]$ ground state. While the emissive state is ligand-field in character, for the tmc complex (tmc = 1,4,8,11-tetramethyl-1,4,8,11-tetraazacyclotetradecane) the only relatively intense electronic transitions observed are those with distinct vibronic structure at 300 (spin allowed) and 350 nm (spin forbidden) which arise from oxo-to-Os(VI) charge-transfer absorption. Although not observed for the tmc complex, the ligand-field transition $(d_{xy})^2 \rightarrow (d_{xy})^1(d^*_\pi)^1$ ($d^*_\pi = d_{xz}, d_{yz}$) is observed for the tetracyano complex.[10] At 80 K, the vibrationally resolved, spin-forbidden absorption $^1A_{1g} \rightarrow {}^3E_g$ ($\nu_{max} \sim 18\,000$ cm^{-1}) and emission ($\nu_{max} \sim 14\,300$ cm^{-1}) are both observed and the 0–0 bands intersect at 16 000 cm^{-1}. The absorption spectra of many (amine)dioxoosmium(VI) complexes are very similar, but very few emit.[8] The red emission observed for the tmc complex has been attributed to the B_{1g} or B_{2g} sublevel of ^3E_g.[8,9] From the ground state $Os^{VI}O_2/Os^{V}O_2$ reduction potential (0.01 V vs NHE[11]) and an ^3E_g excited-state energy of >2 eV, Che and colleagues estimated that $*E°(*Os^{VI}O_2/Os^{V}O_2)$ > 2 V vs NHE in water.[8] Consistent with this high reduction potential, $*Os^{VI}(tmc)O_2^{2+}$ emission is efficiently quenched by amines and sulfides[8] and by aromatic hydrocarbons.[12]

Among the species that are chemically compatible with the dioxoosmium(VI) complex, transparent in the region where it absorbs and may reductively quench its emission, are inorganic

* Abstract published in *Advance ACS Abstracts*, August 15, 1993.

(1) Luong, J. C.; Nadjo, L.; Wrighton, M. S. *J. Am. Chem. Soc.* **1978**, *100*, 5790–5795.
(2) Juris, A.; Balzani, V.; Barigelletti, F.; Campagna, S.; Belser, P.; von Zelewsky, A. *Coord. Chem. Rev.* **1988**, *84*, 85–277.
(3) Hoffman, M. Z.; Bolletta, F.; Moggi, L.; Hug, G. L. *J. Phys. Chem. Ref. Data* **1989**, *18*, 219–543.
(4) Ballardini, R.; Varani, G.; Indelli, M. T.; Scandola, F.; Balzani, V. *J. Am. Chem. Soc.* **1978**, *100*, 7219–7223.
(5) Paulson, S.; Sullivan, B. P.; Caspar, J. V. *J. Am. Chem. Soc.* **1992**, *114*, 6905–6906.
(6) Billing, R.; Zakharova, G. V.; Atabekyan, L. S.; Hennig, H. *J. Photochem. Photobiol. A: Chem.* **1991**, *59*, 163–174.
(7) Mohammed, A. K.; Maverick, A. W. *Inorg. Chem.* **1992**, *31*, 4441–4443.
(8) Che, C.-M.; Yam, V. W.-W.; Cho, K.-C.; Gray, H. B. *J. Chem. Soc., Chem. Commun.* **1987**, 948–949.
(9) Winkler, J. R.; Gray, H. B. *Inorg. Chem.* **1985**, *24*, 346–355.
(10) Sartori, C.; Preetz, W. *Z. Naturforsch.* **1988**, *43a*, 239–247.
(11) Che, C. M.; Poon, C.-K. *Pure Appl. Chem.* **1988**, *60*, 1201–1204.
(12) Che, C.-M.; Cheng, W.-K.; Yam, V. W.-W. *J. Chem. Soc., Dalton Trans.* **1990**, 3095–3100.

0020-1669/93/1332-4200$04.00/0

anions X^- such as the halides and pseudohalides, for which the $X^{\bullet}/X^-$ reduction potentials range from +1.04 V (NO_2^-) to above 2.4 V (Cl^-, SO_4^{2-})[13] and aqua ions such as $Fe(H_2O)_6^{2+}$ and Ce^{III}-(aq). Reductive quenching of strongly oxidizing excited states by simple inorganic reductants has previously been studied in $U^{VI}O_2$ systems[6] and in certain organic systems, such as the triplet states of xanthone,[14] napthoquinone and benzophenone derivatives,[15] and duroquinones.[16] Here we report the results of our studies of $^*Os^{VI}(tmc)O_2^{2+}$ emission quenching by these simple reductants.

Experimental Section

Materials and Methods. Osmium tetroxide was from Alfa Products. $Na_2[OsCl_6]$ was obtained by ion exchange of $(NH_4)_2[OsCl_6]$[17] (Dowex cation-exchange resin AG 50W-X2, 200–400 mesh, Na^+ form, Bio Rad Laboratories). Tin foil and tetramethylcyclam (tmc) were from Aldrich. $[OsO_2(tmc)](PF_6)_2$ was synthesized from $Na_2[OsCl_6]$, and tetramethylcyclam was synthesized according to the literature.[12] Tetrabutylammonium chloride (tbaCl) was from Fluka AG. $(tba)_2[OsO_2(CN)_4]$ and $K_2[OsO_2(CN)_4]$ were prepared from $K_2[OsO_2(OH)_4]$[18] according to the literature.[19] The osmium compounds were stored over Drierite in a refrigerator. Water was purified by a Millipore system. Acetonitrile for spectroscopy was of spectronic grade and, for electrochemistry, of HPLC grade (stored over molecular sieves, 5 Å). The lithium salt of trifluoromethanesulfonic acid was from Aldrich and used without further purification. All other reagents and solvents were of commercially available reagent grade quality. UV–vis spectra were measured in 1-cm quartz cells with (0.1–1) × 10^{-3} M solutions on a Hewlett Packard 8452 A spectrophotometer. ^1H and ^{13}C NMR spectra were recorded on a Bruker AM-300 300-MHz spectrometer. IR spectra were determined on a Mattson Polaris FT-IR spectrometer. Elemental analyses were performed by E. Norton, Brookhaven National Laboratory.

Electrochemistry. Cyclic voltammetry (CV) and differential-pulse voltammetry (DPV) were performed with a BAS 100 instrument at 22 ± 2 °C with a (CV) scan rate of 100 mV s^{-1}, (DPV) pulse height of −10 to −50 mV, and a scan rate of 4 mV s^{-1}. The solutions studied contained 0.1 mM osmium complex and 0.1 M tetrapropylammonium hexafluorophosphate in acetonitrile. A conventional H-type cell was used. Glassy carbon, Pt, and SCE were used as working, counter, and reference electrodes, respectively. Ferrocene was added as an internal standard at the end of each run.

Emission Intensity Measurements. The emission from the dioxo osmium(VI) complex was monitored on a Perkin-Elmer Model MPF-4 fluorescence spectrophotometer equipped with a 150-W xenon lamp. Solutions containing the dioxoosmium(VI) complex (0.3 mM) and quencher were excited at 355 nm, and the emission intensity was monitored at 620 nm. For the sample containing sodium nitrite as quencher, the excitation wavelength was 400 nm because sodium nitrite absorbs strongly below 400 nm. All of the measurements were made with 1-cm fluorescence cells, and the solutions were always freshly prepared. The quenchers were added either by micropipet or syringe or alternatively by mixing equal volumes of solutions of the quencher and the osmium(VI) dioxo complex. The ionic strength was kept constant at 0.5 M with the lithium salt of trifluoromethanesulfonic acid. The absorption spectra of the solutions containing $Os^{VI}(tmc)O_2^{2+}$ and quenchers were equal within experimental error to the combined spectra of complex and quencher. Since the excited-state lifetime and the emission intensity were the same under air and argon, most of the measurements were carried out on air-saturated solutions.

Lifetime Measurements. The samples were placed in 1-cm quartz fluorescence cuvettes in a thermostated cell holder maintained at 25 °C. Samples were excited at 355 nm using the third harmonic from an amplified, mode-locked/Q-switched Nd^{3+}-YAG laser. The pulses were of ~50-ps duration, as confirmed by prior streak camera measurements. The sample emission was collected at normal incidence from the sample cell in a straight-through geometry, while the excitation beam was weakly focused at a 7.5° angle through the cell by a 600-mm focal length lens. The emission was collimated and refocused by a 250-mm focal length lens into a DH-10 double monochromator equipped with 1- or 2-mm slits. Color filters were placed in front of the monochromator to block any scattered excitation light. The fluorescence light from the double monochromator was collected at the exit slit by a multimode optical fiber and passed into an instrument room to the photocathode of a Hamamatsu R928 photomultiplier tube (PMT). The R928 detector was contained within a steel Faraday box to reduce noise from the laser firing, and was operated at a total negative high voltage level of −800 to −1200 V from photocathode to anode. The PMT output was dc-coupled at 50 Ω into an HP 54510A digitizing oscilloscope. The oscilloscope maximum sampling rate of 1 gigasample per second allowed a shortest possible time resolution of 1 ns/point. The time resolution was limited by the 2.2 ns rise time of the R928 PMT, giving an effective lower limit of about 4.5 ns without resorting to deconvolution techniques. The data sets of intensity versus time for the fluorescence decays contained 500 points, over the range of 1.0, 2.0, or 5.0 μs. The experiment was controlled by a LabVIEW 2.2 program, and the data were transferred to a Macintosh computer by GPIB interface.

Analysis of the data was by fitting the fluorescence decay curves to single or double exponential functions using a nonlinear least-squares algorithm in the Igor graphics software. In all cases, three or more decay curves were measured, and the fluorescence rates from the fits were averaged. A check of the system calibration was done by measuring the known lifetime of $Ru(bpy)_3Cl_2$. At 25 °C with 355-nm excitation and 605-nm detection, the lifetime of the Ru complex was 590 ns when fit to a single exponential.

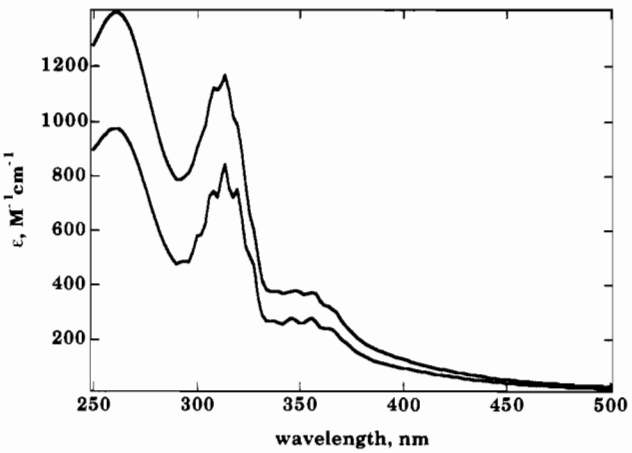

Figure 1. UV/vis spectra of $[Os(tmc)O_2](PF_6)_2$ in water. For comparison the UV/vis spectrum of $[Os(tmc)O_2](PF_6)_2$ in acetonitrile is shown below the spectrum with ε divided by 1.5.

Results

Synthesis. The synthesis of the osmium complexes is straightforward, and the elemental analyses were in accord with the calculated values. For the $[OsO_2tmc](PF_6)_2$ the yield is low, but attempts to improve the method failed. Some black powder, probably OsO_2, formed during the synthesis. $(tba)_2[OsO_2(CN)_4]$ can by synthesized in good yield, but care must be taken that the cyanide groups are not oxidized (additional peak[19] for the bound cyanate at 2230 cm^{-1}) during preparation. Only low yields of $K_2[OsO_2(CN)_4]$ could be obtained. Generally, none of the osmium compounds including the starting materials were stable over time, especially in solution.

Spectral Properties. The UV–vis and IR spectra of $[OsO_2(tmc)](PF_6)_2$ and $(tba)_2[OsO_2(CN)_4]$ are identical with those reported in the literature.[19,20] The UV–vis spectrum of $[OsO_2(tmc)](PF_6)_2$ in water exhibits much less vibrational fine structure than that in acetonitrile (Figure 1), but molar absorptivity and wavelength maximum values are the same in the two solvents. While the molar absorptivity of $OsO_2(tmc)^{2+}$ was comparable to

(13) Stanbury, D. M. *Adv. Inorg. Chem.* **1989**, *33*, 69–138.
(14) Abdullah, S. A.; Kemp, T. J. *J. Chem. Soc. Perkin Trans. 2* **1985**, 1279–1283.
(15) Loeff, I.; Goldstein, S.; Treinin, A.; Linschitz, H. *J. Phys. Chem.* **1991**, *95*, 4423–4430.
(16) Martins, L. J. A. *J. Chem. Soc., Faraday Trans. 1* **1982**, *78*, 533–543.
(17) Dwyer, F. P.; Hogarth, J. W. *Inorg. Synth.* **1957**, *5*, 206–207.
(18) Malin, J. M. *Inorg. Synth.* **1980**, *20*, 61–62.
(19) Preetz, W.; Satori, C. *Z. Naturforsch.* **1988**, *43b*, 94–98.
(20) Yam, V. W.-W.; Che, C.-M. *J. Chem. Soc., Dalton Trans.* **1990**, 3741–3746.

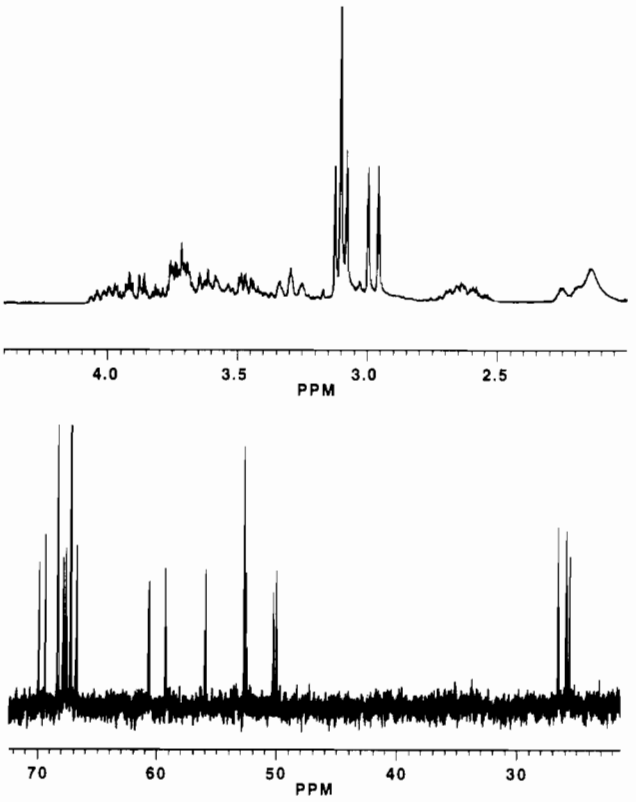

Figure 2. (a, top) ^{1}H-NMR and (b, bottom) ^{13}C-NMR spectra of $[Os(tmc)O_2](PF_6)_2$ in CD_3CN at 25 °C.

that of $OsO_2(CN)_4^{2-}$ in the 500–800-nm region, the spectrum of the tmc complex was featureless in this region. The ^{1}H and ^{13}C NMR spectra of $[OsO_2tmc](PF_6)_2$ in CD_3CN are presented in Figure 2.

Electrochemistry. Cyclic voltammograms of 1 mM $[OsO_2(tmc)](PF_6)_2$ in CH_3CN containing $tba(PF_6)$ exhibited three quasi-reversible couples. The first two, the Os(VI)/Os(V) and Os(V)/Os(IV) couples at –0.29 (1) and –1.36 (1) V vs SCE (–0.67 and –1.73 V, respectively, vs Fc^+/Fc; Fc^+/Fc, +377 mV vs SCE), were reported previously,[21] but our value for the Os(VI)/Os(V) couple is somewhat higher. We also observed an additional couple in the cyclic voltammogram at –2.40 V vs ferrocene. The position of Os(V)/Os(IV) couple is very sensitive to the presence of water: with ca. 2% added water, both cathodic and anodic peaks shifted about 300 mV cathodic of their positions in dry acetonitrile, while the Os(VI)/Os(V) couple shifted only about 15 mV cathodic of its position in the dry solvent.

Emission Studies. An emission-time profile for $[OsO_2(tmc)](PF_6)_2$ in water is shown in Figure 3. Our results for $[OsO_2(tmc)](PF_6)_2$ in water and acetonitrile and for $(tba)_2[OsO_2(CN)_4]$ in acetonitrile are in agreement with published lifetimes.[20] Unfortunately, $K_2[OsO_2(CN)_4]$ did not emit detectably in aqueous solutions and was therefore not suitable for quenching studies in water. Winkler and Gray found that the isoelectronic *trans*-$K[ReO_2(CN)_4]$ is similarly quenched in water.[9]

Most of the quenching measurements were made in aqueous 0.5 M lithium trifluoromethanesulfonate (TFMS). The emission profiles of $OsO_2(tmc)^{2+}$ in these solutions exhibited biexponential behavior with an 8-ns and a 1-μs component. Careful examination excluded the solvent, cuvettes, lenses, and filters as source of the 8-ns component. The fast component was observed whenever LiTFMS was present, but was absent when no salt was added or sodium chloride was used instead of the triflate. The emission from the LiTFMS was peaked at 550 nm, but still had substantial intensity at 610–620 nm, where the Os emission was monitored.

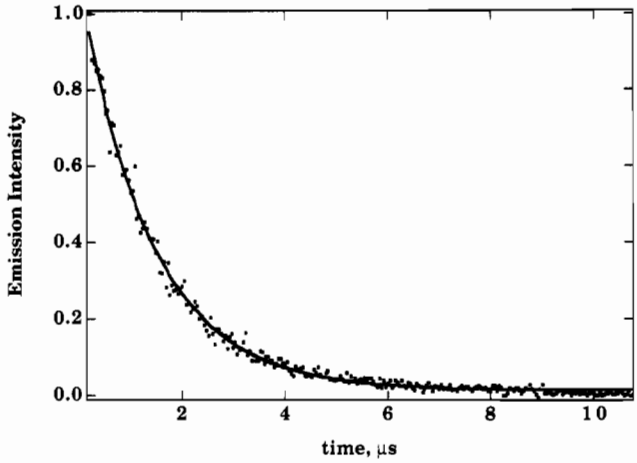

Figure 3. Decay of the 620-nm emission of the excited state of $[Os(tmc)O_2](PF_6)_2$ in water at 25 °C, [complex] = 3×10^{-4} M, and excitation at 355 nm.

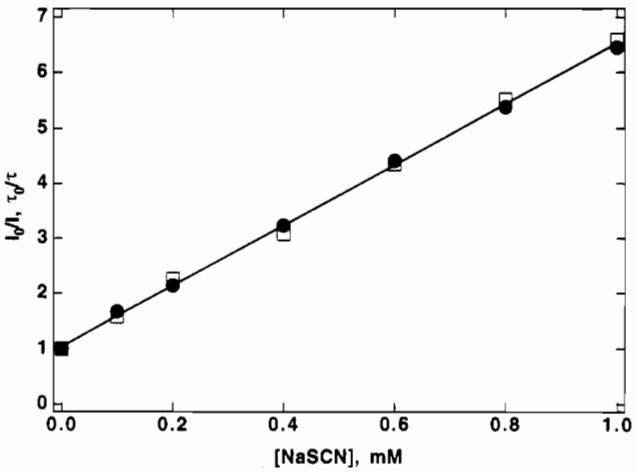

Figure 4. Stern–Volmer plot for quenching of the $^*Os(tmc)O_2^{2+}$ emission by NaSCN in 0.5 M $Li(CF_3SO_3)$ at 25 °C: circles, intensity quenching; squares, lifetime quenching.

Emission with a similar lifetime (but of smaller amplitude) was observed for KTFMS or triflic acid. Thus the emission is due to an impurity in commercial triflate. The longer lived component is due to the single exponential decay of the $OsO_2(tmc)$ complex. The lifetime of the excited state of $[OsO_2(tmc)](PF_6)_2$ under the conditions in which the quenching measurements were made (0.5 M LiTFMS, 0.3 mM complex) is (1.0 ± 0.1) μs.

The quenching of the emission of the excited state of the dioxoosmium complex by the inorganic salts studied gave good linear relationships (intercept unity) when I_0/I or τ_0/τ was plotted against quencher concentration. The slope of such a plot is the Stern–Volmer constant K_{SV}, and the bimolecular quenching rate constant k_q is obtained from the relationship $k_q = K_{SV}/\tau_0$ where τ_0 is the lifetime of the excited state in the absence of quencher (1.0 ± 0.1 μs). The Stern–Volmer plot for thiocyanate quenching is shown in Figure 4, in which the agreement between the results of time-resolved and intensity measurements is excellent. Most of the quenching data were therefore obtained by intensity measurements on the spectrofluorimeter. A summary of the quenching data is given in Table I, along with literature values of the quencher reduction potentials.[13,22,23]

Transient absorption measurements were attempted on carbonate (20 mM)/$Os^{VI}(tmc)O_2^{2+}$ (0.3 mM) solutions in an effort to detect the electron-transfer product $^*CO_3^-$, which has an

(21) Che, C. M.; Cheng, W. K. *J. Chem. Soc., Chem. Commun.* **1986**, 1519–1521.

(22) Huie, R. H.; Clifton, C. L.; Neta, P. *Int. J. Radiat. Appl. Instrum., Part C* **1991**, *38*, 477–481.

(23) Latimer, W. M. *Oxidation Potentials*; 2nd ed., Prentice-Hall: Englewood Cliffs, NJ 1954; p 345.

Table I. Rate Constants for Emission Quenching of *trans*-$[Os(tmc)O_2]^{2+}$ at 25 °C[a]

	quencher salt	k_q, M^{-1} s^{-1} intensity	k_q, M^{-1} s^{-1} lifetime	$E°(Q^+/Q)$, V vs NHE[b]
1	Na_2SO_4	$\leq 1 \times 10^5$		2.43
2	NaCl	4×10^5		2.41
3	$TlClO_4$	3×10^5		2.22
4	$NaHCO_2$	1.5×10^6		2.0
5	$AgClO_4$[c]	1.7×10^8		1.98
6	NaBr	1.6×10^8	1.7×10^8	1.92
7	NaOH	1×10^7		1.89
8	$Co(ClO_4)_2$	1×10^6		1.84
9	NaSCN	5.5×10^9	5.6×10^9	1.63
10	$Ce^{III}(ClO_4)_3$	$\leq 1 \times 10^5$		1.61
11	Na_2CO_3	1.5×10^8	1.6×10^8	1.59
12	$Ce^{III}(SO_4)^+$[d]	1.0×10^7		1.44
13	NaN_3	4.9×10^9	4×10^9	1.33
14	NaI	6.4×10^9	6.5×10^9	1.33
15	$NaNO_2$	2×10^9		1.04
16	$(NH_4)_2Fe(SO_4)_2$	1×10^9		0.77
17	$NaHCO_3$	8×10^6		

[a] *trans*-$[Os(tmc)O_2](PF_6)_2$ = 3×10^{-4} M; [quencher] = 0.0001–0.02 M; ionic strength = 0.5 M $LiCF_3SO_3$; λ (excitation) = 355 nm; λ (emission) = 620 nm. Estimated errors for quenching rate constants: ±10%. [b] Reduction potentials from the literature. $Ag^{II/I}$, $Ce^{IV/III}$: Latimer, W. M. *Oxidation Potentials*, 2nd Ed., Prentice-Hall, Englewood Cliffs, NJ, 1954, p 345; $(CO_3^{-/2-}$ and $SO_4^{2-/-})$: Huie, R. H.; Clifton, C. L.; Neta, P. *Int. J. Radiat. Appl. Instrum., Part C* **1991**, *38*, 477–481. $HCO_2^{-/0}$: Billing, R.; Zakharova, G. V.; Atabekyan, L. S.; Hennig, H. *J. Photochem. Photobiol. A: Chem.* **1991**, *59*, 163–174. Remaining data are from Stanbury, D. M. *Adv. Inorg. Chem.* **1989**, *33*, 69–138. [c] In 0.5 M CF_3SO_3H. [d] In 0.5 M H_2SO_4.

absorption maximum at 600 nm ($\epsilon = 1.9 \times 10^3$ M^{-1} cm^{-1}).[22] No transient $^{\bullet}CO_3^-$ absorption was observed (yield ≤ 0.05).

Other Complexes Surveyed. Synthesis of the tetramethylethylenediamine complex $[OsO_2(Me_4en)_2](PF_6)_2$ was attempted in the hope that replacement of all of the amine N–H groups of $OsO_2(en)_2^{2+}$ with N–Me groups would lengthen the lifetime of the ligand-field excited state in solution. A small amount of emissive, yellow solid was obtained[18] but decomposed rapidly in water, and no emission was observed for the aqueous solution. Perchlorate salts of $OsO_2L_2^{2+}$ with L = ethylenediamine or propylenediamine were found to emit in the solid state.

Discussion

Isomerism. Complexes of tetramethylcyclam form several isomers. From the extensive work on the nickel complexes of this ligand,[24-26] the most likely isomers for $OsO_2(tmc)^{2+}$ are **A**–**C**.

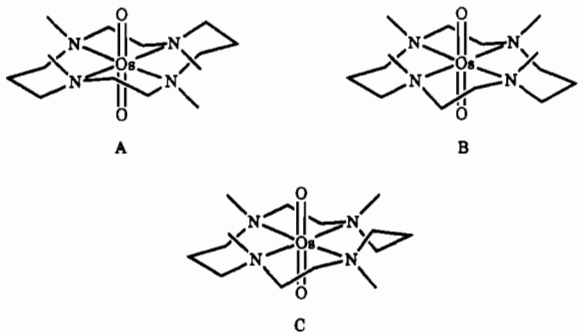

A **B**

C

For oxoruthenium(IV) complexes, analogues of all three isomers have been characterized by X-ray crystallography.[27] Isomers **A** and **B** should exhibit a single methyl peak in the ^{1}H-NMR spectrum, while four methyl signals should be observed for **C**. Since five methyl signals are found (see Figure 2a), it is clear that a mixture of isomers is present. This is confirmed by the ^{13}C-NMR in Figure 2b in which more than 14 individual carbon resonances are evident. The major component of the isomer mixture must be isomer **C**, while the most likely minor isomer is **B**, in accordance with the findings for the nickel complexes of tmc. All efforts to separate the isomers or to obtain one single isomer were unsuccessful. Thus it is possible that the isomers interconvert relatively rapidly on Os(VI), perhaps via an η^3 form of the complex. No evidence for two emitting $OsO_2(tmc)^{2+}$ species was found in the time or wavelength profile of the emission. Thus, either only one isomer emits or the two isomers have very similar excited-state lifetimes and quenching rate constants.

The $OsO_2(tmc)^{2+}$ Excited State. As has been noted by others,[8] the OsO_2 chromophore (which is dominated by the oxygen-to-metal charge-transfer bands) is insensitive to the nature of the amine ligand. Thus the absorption spectrum of the tmc complex is virtually identical to that of the tetraammine, the bis(ethylene)-diamine, etc. complexes.[8] However, the latter do not emit in solution at room temperature. The methylation of the amine groups in the tmc complex thus appears implicated in lengthening the lifetime of the emissive d–d state by reducing its nonradiative decay rate. The tmc ligand has also attracted interest because it stabilizes low oxidation states of transition metals (for example, upon *N*-methylation of cyclam, the Cr(III)/Cr(II) potential shifts more than +1 V[28] and the Ru(III)/Ru(II) potential shifts ca. +400 mV[29]). However, as in the present system, high oxidation states are also stabilized. Explanations considered[28] for the stabilization of low oxidation states by N-methylation include (1) the nitrogens becoming poorer σ-donors, (2) the increased cavity size more readily accommodating the (larger radius) low oxidation state, (3) the decreased solvation of the complex produced by the hydrophobic methyl groups. Of these, the diminished solvation and the absence of N–H groups are likely the most important factors in lengthening the lifetime of the tmc complex.

The insensitivity of the *trans*-dioxoosmium(VI) chromophore to environment (the nature of the equatorial ligands) also extends, for the tmc complex, to insensitivity to solvent: the absorption and emission maxima are virtually the same in water and in acetonitrile. However, interestingly, the vibrational fine structure in the absorption spectrum is not as resolved in water as in acetonitrile (Figure 1), possibly because of interaction of the oxo groups with solvent protons.

Self-Quenching. The $^{*}Os^{VI}(tmc)O_2^{2+}$ emission is quenched by the ground-state complex. The self-quenching process ($k = 2.6 \times 10^9$ M^{-1} s^{-1})[12] is sufficiently rapid that it is an important experimental consideration and the mechanism of the process is of some interest. A mechanism involving exciplex formation has been invoked for self-quenching of polypyridylchromium(III) ligand-field excited states.[30] By contrast, $Ru(bpy)_3^{2+}$ and other MLCT states do not self-quench detectably. For nitridoosmium(VI) complexes, a self-quenching mechanism involving interaction of the nitrides on ground- and excited-state complexes has been proposed.[31] It is difficult to see how such a mechanism would apply to the dioxo systems. Indeed, a proton-quenching mechanism (involving the ammine hydrogens) seems more reasonable for the nitrido systems, since they are known to be very effectively quenched by proton sources. One mechanism to be considered for the $^{*}Os^{VI}(tmc)O_2^{2+}$ self quenching is the redox mechanism

(24) Barefield, E. K.; Wagner, F. *Inorg. Chem.* **1973**, *12*, 2435–2439.
(25) Moore, P.; Sachinidis, J.; Willey, G. R. *J. Chem. Soc., Chem. Commun.* **1983**, 522–523.
(26) Lincoln, S. F.; Coates, J. H.; Hadi, D. A.; Pisaniello, D. L. *Inorg. Chim. Acta* **1984**, *81*, L9–L10.
(27) Che, C.-M.; Lai, T.-F.; Wong, K.-Y. *Inorg. Chem.* **1987**, *26*, 2289–2299.
(28) Guldi, D.; Wasgestian, F.; Meyerstein, D. *Inorg. Chim. Acta* **1992**, *194*, 15–22.
(29) Che, C. M.; Wong, K.-Y.; Poon, C.-K. *Inorg. Chem.* **1986**, *25*, 1809–1813.
(30) Serpone, N.; Hoffman, M. Z. *J. Chem. Educ.* **1983**, *60*, 853–860.
(31) Lam, H.-W.; Che, C.-M.; Wong, K.-Y. *J. Chem. Soc., Dalton Trans.* **1992**, 1411–1416.

(eq 1) which results in disproportionation to Os(VII) and Os(V).

$$*Os^{VI}O_2(tmc)^{2+} + Os^{VI}O_2(tmc)^{2+} \rightarrow Os^{V}O_2(tmc)^{+} + Os^{VII}O_2(tmc)^{3+} \quad (1)$$

The free-energy change for eq 1 is obtained from the difference between $*Os^{VI}/Os^{V}$ and Os^{VII}/Os^{VI} reduction potentials. The latter couple has not been characterized and no redox processes are observed for $OsO_2(tmc)^{2+}$ between –0.3 V (the Os^{VI}/Os^{V} couple) and +1 V vs SCE in acetonitrile. Thus $\Delta G° \leq -1.3$ eV, but the $\Delta G°$ could be favorable even if the Os^{VII}/Os^{VI} couple lies near the cathodic solvent limit.

The $*Os^{VI}(tmc)O_2/Os^{V}(tmc)O_2$ Excited-State Couple. The emission maximum of the tmc complex in acetonitrile at room temperature is 620 nm[8] (1.97 eV) and the 0–0 band has been estimated to lie at 2.25 eV.[20] The latter value, taken with the ground-state reduction potential in water (+0.01 V vs NHE[11,12,32,33]), places the excited-state reduction potential estimate at +2.26 V vs NHE in water, the value that will be used here. From studies of the reductive quenching by aromatic hydrocarbons, Yam and Che[20] have proposed the value +2.39(10) V vs NHE for the excited-state couple in acetonitrile. However, the latter value is based on an inappropriate correction of the electrochemical values obtained for the aromatic couples[34,35] in acetonitrile and should be 2.23(10) V.

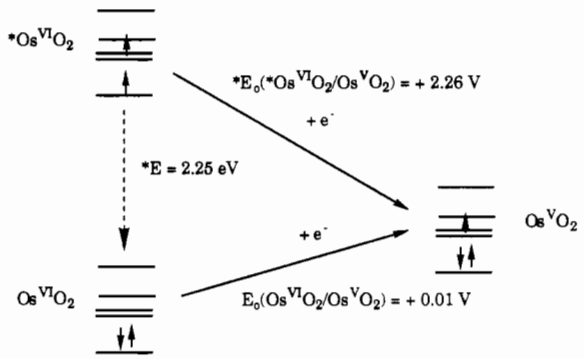

The intrinsic barrier to outer-sphere electron transfer for the $*Os^{VI}(tmc)O_2/Os^{V}(tmc)O_2$ couple is comprised of inner-shell (λ_{in}) and outer-shell (solvent, λ_{out}) contributions.[36] λ_{in} should be quite small, since the change in Os–O distance between ground and excited states inferred[10] from the spectroscopy of the tetracyano complex is only 0.010–0.013 Å. However, to the extent that the oxo groups of Os(VI) and Os(V) interact differently with solvent (stronger hydrogen-bonding to water for the lower oxidation state), some contribution to λ_{in} is expected in water. The magnitude of λ_{out} is estimated to be 1.20 eV with use of a mean-sphere radius approximation.[37] (The values 4.2, 4.2, and 2.0 Å were used for the Os–macrocycle and Os–O radii, respectively. On the basis of the structure of $Os(en)_2O_2^{2+}$,[38] the Os–O and Os–N distances are expected to be 1.74 and 2.11 Å, respectively). Thus the self-exchange rate constant for the couple would be 1×10^7 M^{-1} s^{-1} at 25 °C if only outer-shell contributions were significant.[39,40] The self-exchange rate for the ground-state $Ru^{VI}(tmc)O_2/Ru^{V}(tmc)O_2$ couple has been estimated to be 1.5×10^5 M^{-1} s^{-1} at 25 °C.[41] Here the value 1×10^5 M^{-1} s^{-1} will be used for the $*Os^{VI}(tmc)O_2/Os^{V}(tmc)O_2$ couple.

Table II. Comparison of Calculated Electron-Transfer Rate Constants with the Observed Quenching Rate Constants (k_q) for Aqua Ions[a]

Q	k_{11},[b] M^{-1} s^{-1}	r_Q, Å	k_{calc},[c] M^{-1} s^{-1}	k_q, M^{-1} s^{-1}
$Fe(H_2O)_6^{2+}$	4.2	3.3	2.0×10^9	1.0×10^9
$Ce^{III}(SO_4)^{+}$	4.0	3.5	1.7×10^8	1.0×10^7
$Co(H_2O)_6^{2+}$	5	3.3	1.5×10^6	1.0×10^6
Ag^{I}	2×10^4 [d]	3.3	6.3×10^6	1.7×10^8
Tl^{I}	1.5×10^4 [e]	3.3	8.4×10^4	3.0×10^5

[a] Calculated from[36] $k_{12} = (k_{11}k_{22}K_{12}f_{12})^{1/2}W_{12}$; $\log f_{12} = (\log K_{12})^2/4\log(k_{11}k_{22}/10^{22})$ with $k_{22} = 1 \times 10^5$ M^{-1} s^{-1} and $*E° = +2.26$ V vs NHE and the quencher reduction potential listed in Table I. The calculated values have been corrected for f factors and work terms. The quencher radius is r_Q; the radius used for the excited state is 3.3 Å. [b] Self-exchange rate constants: Sutin, N. *Annu. Rev. Nucl. Sci.* **1962**, *12*, 285–328. [c] In correcting k_{calc} for diffusion, $k_{diff} = 2 \times 10^9$ M^{-1} s^{-1} was used. [d] Calculated from the data given in Huchital, D. H.; Sutin, N.; Warnquist, B. *Inorg. Chem.* **1967**, *6*, 838–840. [e] Schwarz, H. A.; Comstock, D.; Yandell, J. K.; Dodson, R. W. *J. Phys. Chem.* **1974**, *78*, 488–493.

Excited-State Quenching. The reagents used in this study were selected because of their reducing properties, with the expectation that reductive quenching (eq 2) would occur. Electron-transfer

$$*Os^{VI}(tmc)O_2^{2+} + Q \rightarrow Os^{V}(tmc)O_2^{+} + Q^{+} \quad (2)$$

quenching is the only possible mechanism for most of the reagents used, since their spectroscopy precludes energy-transfer quenching mechanisms. (However, $Fe(H_2O)_6^{2+}$ and $Co(H_2O)_6^{2+}$ are exceptions since they have ligand field states in the relevant region of the spectrum). In Table II, k_q values are compared with calculated rate constants (k_{12}) for electron transfer for the aqua ion quenchers. The latter are obtained from eq 3,[36,42] where K_{12}

$$k_{12} = (k_{11}k_{22}K_{12}f_{12})^{1/2}W_{12} \quad (3a)$$

$$\log f_{12} = \frac{(\log K_{12})^2}{4 \log\left(\frac{k_{11}k_{22}}{10^{22}}\right)} \quad (3b)$$

is the equilibrium constant for electron transfer (eq 2), k_{11} is the

(32) The electrochemistry of $Os^{VI}(tmc)O_2$ in water is complex because of the protonation processes which accompany its reduction.[11,12] However, the $Os^{VI}(tmc)O_2/Os^{V}(tmc)O_2$ couple has been reported to undergo reversible one-electron transfer above pH 8, with a reduction potential of +0.02 V vs NHE.[11,12] From cyclic voltammetry in acetonitrile the ground-state Os(VI)/Os(V) reduction potential is –0.67 V vs Fc^+/Fc. Assuming the Fc^+/Fc potential to be solvent independent and using +0.38 V vs NHE as the Fc^+/Fc reduction potential in water, the value –0.30 V vs NHE would be estimated for the $Os^{VI}(tmc)O_2/Os^{V}(tmc)O_2$ couple in water. Thus the potential appears to be very solvent sensitive. For the ruthenium analog, a similar sensitivity has been observed,[33] and the data suggest that the couple increases in oxidizing strength as the acceptor number of the solvent increases. Such effects can result from preferential hydrogen bonding to the lower oxidation state (Ru(V) or Os(V)), consistent with the greater basicity of the oxo groups on the V oxidation state (e.g., $pK(Ru^{VI}(tmc)O_2) < 1$; $pK(Ru^{V}(tmc)O_2) \sim 1$).

(33) Che, C.-M.; Wong, K.-Y.; Anson, F. C. *J. Electroanal. Chem.* **1987**, *226*, 211–226.

(34) In the original study of the aromatic hydrocarbons (Howell, J. O.; Goncalves, J. M.; Amatore, C.; Klasinc, L.; Wightman, R. M.; Kochi, J. K. *J. Am. Chem. Soc.* **1984**, *106*, 3968–3976) values obtained in acetonitrile vs SCE were corrected to NHE by adding 0.24 V (SCE vs NHE in water); in reality the liquid junction effectively cancels the 0.24-V value. (See: Bock, C. R.; Connor, J. A.; Gutierrez, A. R.; Meyer, T. J.; Whitten, D. G.; Sullivan, B. P.; Nagle, J. K. *J. Am. Chem. Soc.* **1979**, *101*, 4815–4824.) In light of the indications that $Os^{VI}(tmc)O_2^{2+}$ is a much weaker oxidant in acetonitrile, it is difficult to reconcile the electrochemistry with the results of the quenching analysis.

(35) Howell, J. O.; Goncalves, J. M.; Amatore, C.; Klasinc, L.; Wightman, R. M.; Kochi, J. K. *J. Am. Chem. Soc.* **1984**, *106*, 3968–3976.

(36) Macartney, D. H.; Sutin, N. *Inorg. Chem.* **1985**, *24*, 3403–3409.

(37) Brown, G. M.; Sutin, N. *J. Am. Chem. Soc.* **1979**, *101*, 883–892.

(38) Malin, J. M.; Schlemper, E. O.; Murmann, R. K. *Inorg. Chem.* **1977**, *16*, 615–619.

(39) From the analysis of the quenching data in acetonitrile,[12] $\lambda = 0.75$ eV for the $Os^{VI}(tmc)O_2$/aromatic cross reaction. Taking $\lambda(Ar) = 0.62$ eV for the aromatic (assuming that $\lambda(Ar)$ is the same as for nitroaromatic quenchers[40]), $\lambda(Os) = 0.98$ eV in acetonitrile.

(40) Bock, C. R.; Connor, J. A.; Gutierrez, A. R.; Meyer, T. J.; Whitten, D. G.; Sullivan, B. P.; Nagle, J. K. *J. Am. Chem. Soc.* **1979**, *101*, 4815–4824.

(41) Che, C.-M.; Lau, K.; Lau, T.-C.; Poon, C.-K. *J. Am. Chem. Soc.* **1990**, *112*, 5176–5181.

(42) Chou, M.; Creutz, C.; Sutin, N. *J. Am. Chem. Soc.* **1977**, *99*, 5615–5623.

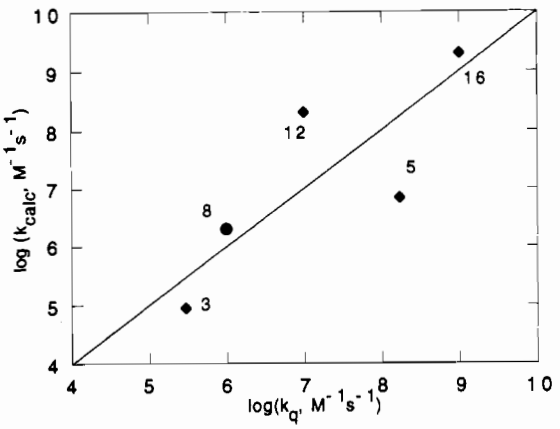

Figure 5. Comparison of calculated electron-transfer (k_{12}) rate constants and observed k_q values for quenching of $*Os(tmc)O_2^{2+}$ by aqua ions. The points are numbered as in Table I.

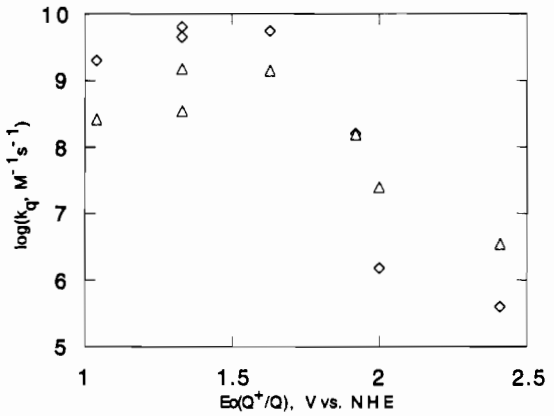

Figure 6. Comparison of quenching rate constants for $*UO_2F_4^{2-}$ (triangles) and $Os(tmc)O_2^{2+}$ (diamonds) with (left to right) nitrite, azide, iodide, thiocyanate, bromide, formate, and chloride ions.

self-exchange rate constant for the quencher Q/Q^+ couple,[43,44] k_{22} is the self-exchange rate for the $*Os^{VI}(tmc)O_2/Os^{V}(tmc)O_2$ couple (1.0×10^5 M^{-1} s^{-1}), and the work-term corrections were made as given elsewhere.[36] The value for $Fe(H_2O)_6^{2+}$ has also been corrected for the effects of diffusion control through the relation, $(k_q)^{-1} = (k_{12})^{-1} + (k_{diff})^{-1}$, with $k_{diff} = 2 \times 10^9$ M^{-1} s^{-1}. The observed and calculated values are compared in Figure 5. The agreement between observed and calculated rate constants is comparable to that usually observed in outer-sphere reactions.[42] However, points 3 and 4 are unusual; since the observed k_{12} values are generally systematically lower than those calculated from eq 3[42] and the values calculated for Tl^I and Ag^I quenching are smaller than the observed values, the exchange rate constants used for these couples may be too small.

Anionic Quenchers. The $*Os^{VI}(tmc)O_2^{2+}$ data can be compared with results reported for $UO_2F_4^{2-}$ excited-state quenching.[6] As shown in Figure 6, the $*Os^{VI}(tmc)O_2^{2+}$ data track the $*UO_2F_4^{2-}$ data fairly consistently. Excited-state charge type favors the OsO_2^{2+} reactions with the uninegatively charged quenchers by about a factor of 2 at 0.5 M ionic strength, at which both studies were performed. The reduction potential of the $*UO_2F_4^{2-}/UO_2F_4^{3-}$ couple is greater (+2.6 V vs NHE), but its self-exchange rate constant is smaller (1–10 M^{-1} s^{-1}, based on the ground-state couple[45]), and its reactions may be nonadiabatic.[6,45]

The intrinsic reactivity of couples involving small anions with respect to outer-sphere electron transfer has attracted attention in recent years.[43,46–50] These couples are of interest in several areas, including radiation chemistry and photochemistry. The species range from the monatomic halides, to linear triatomics (azide and thiocyanate), to bent triatomics (nitrite, chlorite), to tetraatomic and larger species (carbonate, formate, higher carboxylates) and raise a number of interesting issues: In considering the apparent self-exchanges of the halide/halogen couples, the possibility that these reagents lie in the strong (electronic) coupling limit has been raised. By contrast, the reactivity of the N_3^-/N_3 couple appears consistent with modest electronic coupling and a barrier dominated by outer-shell reorganization.[50] For the bent triatomics, changes in bond angles contribute significantly to the inner-shell barrier.[47]

In assessing the outer-sphere reactivity of these couples, a number of problems arise, some conceptual and some experimental. One conceptual problem is the definition of radius for a polyatomic species, particularly for species such as nitrite or carbonate. At the experimental level, there are several daunting problems. Attempts to directly evaluate the self-exchange process are frustrated by the intervention of net chemical reactions or the formation of bound intermediates (I_2^-) through which exchange occurs. As a consequence, self-exchange rates have been estimated from net reaction rates with use of the Marcus cross relation. In many instances, the redox potentials of the couples are so high that conventional reagents cannot access them. Because iodide ion is rather easily oxidized, oxidation of iodide ion by ground-state metal complexes has been the most extensively studied. However, as Stanbury et al.,[46] pointed out, in some cases the rate-determining step in the oxidation is not electron transfer, but rather diffusive separation of the reduced metal complex and iodine atom, with the electron-transfer step being a rapid preequilibrium. This situation results from the large endergonicity of the reactions. From analysis of a data set complicated only to a small extent by the latter problem, a self-exchange rate constant of $(2 \pm 1) \times 10^8$ M^{-1} s^{-1} has been inferred for the $*I/I^-$ couple.[48] Analysis of literature data for iodide quenching polypyridylchromium(III) excited states[30] yields an estimate of 1×10^7 M^{-1} s^{-1}.

Self-exchange rates for the inorganic anion couples obtained from the $*Os^{VI}(tmc)O_2^{2+}$ data are presented in Table III. The values were calculated from the $*Os(tmc)O_2^{2+}$ quenching rate constant (k_{12}) using eq 3, with $k_{22} = 1 \times 10^5$ M^{-1} s^{-1}, $*E^\circ$ = +2.26 V vs NHE, and the quencher reduction potential listed. The quencher radius is r_Q; the radius used for the excited state is 3.3 Å. The calculated values have been corrected for f factors and work terms by an iterative fit to k'_q, using the value obtained from the simple cross-relation $k_{11} = (k_{12})^2/(k_{22}K_{12})$ as the initial trial value. With $*Os^{VI}(tmc)O_2^{2+}$ serving as oxidant, electron transfer from all but chloride ion is thermodynamically favorable and so the electron-transfer preequilibrium complication common for ground-state oxidants is eliminated.

For the first three entries in Table III, the quenching rate constants (Table I) are so great that corrections for diffusion control are significant. The k_{11} values given were calculated from the corrected rate constants. Interestingly, the k_{11} values are smaller than the previously reported estimates for all three couples. (Alternatively stated, the $k_{12,calc}$ values obtained with previously reported exchange-rate estimates are larger than the observed rate constants.) This is not an artifact of the diffusion correction: the value $k_{diff} = 1 \times 10^{10}$ M^{-1} s^{-1}, used in making the correction, is at the low end of values implicated for k_{diff}. However, the magnitudes of k_{11} could only be increased by decreasing the

(43) Stanbury, D. M.; Martinez, R.; Tseng, E.; Miller, C. E. *Inorg. Chem.* **1988**, *27*, 4277–4280.
(44) Sutin, N. *Annu. Rev. Nucl. Sci.* **1962**, *12*, 285–328.
(45) Howes, K. R.; Bakac, A.; Espenson, J. H. *Inorg. Chem.* **1988**, *27*, 791–794.
(46) Stanbury, D. M.; Wilmarth, W. K.; Khalaf, S.; Po, H. N.; Byrd, J. E. *Inorg. Chem.* **1980**, *19*, 2715–2722.
(47) Stanbury, D. M.; Lednicky, L. A. *J. Am. Chem. Soc.* **1984**, *106*, 2847–2453.
(48) Fairbank, M. G.; McAuley, A. *Inorg. Chem.* **1987**, *26*, 2844–2848.
(49) Ram, M. S.; Stanbury, D. M. *J. Am. Chem. Soc.* **1984**, *106*, 8136–8142.
(50) Ram, M. S.; Stanbury, D. M. *J. Phys. Chem.* **1986**, *90*, 3691–3696.

Table III. Self-Exchange Rate Constants Calculated from the Quenching Data

couple	$E°(Q^+/Q)$, V vs NHE	r_Q, Å	k_{11}[a], M^{-1} s^{-1}	k_{11}, M^{-1} s^{-1}
$NO_2^{-/0}$	1.04	1.5	5×10^{-6}	3×10^{-2} [b]
$N_3^{-/0}$	1.33	1.5	1×10^3	4×10^4 (10^3 to 10^8) [c]
$I^{-/0}$	1.33	2.16	1×10^4	$(2 \pm 1) \times 10^8$ [c] 10^4–10^9 [c] 1×10^7 [d]
$CO_3^{2-/-}$	1.59	1.5	0.4	0.5 [e]
$Ce^{III/IV}$(aq)	1.61	3.5	$\leq 10^{-6}$	(≤ 0.06) [f]
$SCN^{-/0}$	1.63	1.5	1×10^7	
$OH^{-/0}$	1.89	1.4	3×10^2	3×10^5 [e]
$Br^{-/0}$	1.92	1.95	3×10^5	3×10^7 [e]
$HCO_2^{-/0}$	2.0	1.5	3×10^2	4×10^3 [g]
$Cl^{-/0}$	2.41	1.81	*h*	7×10^8 [g]

[a] Calculated from the $*Os(tmc)O_2^{2+}$ quenching rate constant with [36] $k_{12} = (k_{11}k_{22}K_{12}f_{12})^{1/2}W_{12}$; $\log f_{12} = (\log K_{12})^2/(4 \log (k_{11}k_{22}/10^{22}))$ with $k_{22} = 1 \times 10^5$ M^{-1} s^{-1}, $*E° = +2.26$ V vs NHE, and the quencher reduction potential listed. The quencher radius is r_Q; the radius used for the excited state is 3.3 Å. The calculated values have been corrected for *f* factors and work terms by an iterative fit to k'_q, using the value obtained from the simple cross relation $k_{11} = (k_{12})^2/(k_{22}K_{12})$ as initial trial value. For Q = NO_2^-, N_3^-, I^-, and SCN^-, the k_{12} value measured was corrected for the effects of diffusion control, through the equation, $(k'_q)^{-1} = (k_q)^{-1} - (k_{diff})^{-1}$ with $k_{diff} = 1 \times 10^{10}$ M^{-1} s^{-1}. [b] Ram, M. S.; Stanbury, D. M. *J. Am. Chem. Soc.* **1984**, *106*, 8136–8142. [c] Ram, M. S.; Stanbury, D. M. *J. Phys. Chem.* **1986**, *90*, 3691–3696. [d] The first values are from: Fairbank, M. G.; McAuley, A. *Inorg. Chem.* **1987**, *26*, 2844–2848. The second is from: Stanbury, D. M.; Wilmarth, W. K.; Khalaf, S.; Po, H. N.; Byrd, J. E. *Inorg. Chem.* **1980**, *19*, 2715–2722. The third is from analysis of data given in: Serpone, N.; Hoffman, M. Z. *J. Chem. Educ.* **1983**, *60*, 853–860. [e] Calculated from the quenching rate constant for the triplet state of nitrothiophene,[16] with $k_{11} = (k_{12})^2/(k_{22}K_{12})$, where k_{12} is k_q, k_{22} is 1×10^8 M^{-1} s^{-1}, and K_{12} is calculated from $*E° = +2.18$ V vs NHE and the quencher reduction potential listed. [f] Sutin, N. *Annu. Rev. Nucl. Sci.* **1962**, *12*, 285–328. [g] Calculated from the $*UO_2F_4^{2-}$ quenching rate constant with $k_{11} = (k_{12})^2/(k_{22}K_{12})$, where k_{12} is k_q, k_{22} is 10 M^{-1} s^{-1}, and K_{12} is calculated from $*E° = +2.6$ V vs NHE[6] and the quencher reduction potential listed. [h] Since the reverse rate constant for electron transfer calculated from k_{12}/K_{12} is 3×10^{10} M^{-1} s^{-1}, electron-transfer is not rate determining.

k_{diff} value used in calculating the activation-controlled rate constant. For nitrite, azide, and iodide, the reactions are quite exergonic ($|\Delta G°| \geq 1$ eV), and the f_{12} corrections are significant ($f_{12} = 10^{-5}$–10^{-3}). The discrepancy could then lie in an underestimate of the magnitude of the f_{12} correction. With constant driving force, the magnitude of the f_{12} correction increases with $|\Delta G°/\lambda|$, and the evaluation of λ from rate constants depends upon the value of the preexponential factor.[51] The preexponential factor used in the present calculations was 10^{11} M^{-1} s^{-1}, and there is no reason to reduce its value.

The k_{11} values extracted for iodide and azide couples do actually lie in the range, albeit it at the low end, of values obtained from other cross reaction data. Many of the systems previously studied involved polypyridyl complexes and for these the anion could react at the clefts between the rings (thereby reducing the outer-shell barrier, and perhaps, increasing the electronic coupling, *vide infra*). Thus the X^-/ML_3^{3+} reactions may exhibit a higher effective self-exchange rate. For nitrite ion, an additional factor may be considered. Stanbury and Lednicky[47] proposed that nuclear tunneling makes a substantial contribution to the NO_2/NO_2^- self exchange, enhancing its rate by a factor of 80 at 25 °C. Contributions from nuclear tunneling diminish with increasing $|\Delta G°/\lambda|$ (below $|\Delta G°/\lambda| = 1$).[52] For the present quenching reaction, $|\Delta G°/\lambda|$ lies in the 0–1 range. Thus it is possible the k_{11} value (5×10^{-6} M^{-1} s^{-1}) obtained here provides a measure of the NO_2/NO_2^- self-exchange rate in the absence of nuclear tunneling contributions.

(51) Brunschwig, B.; Sutin, N. *J. Am. Chem. Soc.* **1978**, *100*, 7568–7577.
(52) Sutin, N. *Prog. Inorg. Chem.* **1983**, *30*, 441–498.

Table IV. Comparison of Calculated and Observed Spectral Properties of $Ru(NH_3)_6^{3+}/X^-$ Ion Pairs

	halide (X^-)			
	I^-	Br^-	Cl^-	F^- [e]
λ_{out},[a] eV	1.59	1.70	1.82	2.32
$\Delta E°$, eV	1.28	1.87	2.36	
$\lambda_{out} + \Delta E°$,[b] eV	2.87	3.57	4.18	
E_{op},[a] eV	3.08	3.84	4.22	
λ_{out} ($X·/X^-$)	1.82	2.01	2.11	2.80
$k_{ex}(X·/X^-)$[d]	2×10^3	3×10^2	1×10^2	10^{-1}

[a] Calculated from eq 4. [b] Calculated from the $E°(X·/X^-)$ in Table I, with $E°(Ru(NH_3)_6^{3+/2+}) = +0.05$ V vs NHE, as reported by: Lim, H. S.; Barclay, D. J.; Anson, F. C. *Inorg. Chem.* **1972**, *11*, 1460–1466. [c] E_{op} values for formation of the $^2P_{3/2}$ halogen state reported by Waysbort, D.; Evenor, M.; Navon, G. *Inorg. Chem.* **1975**, *14*, 514–519. [d] Calculated for the self-exchange, neglecting λ_{in}, using eq 4 to evaluate λ_{out} and $K_A\kappa_{el}\nu_n = 10^{11}$ M^{-1} s^{-1}. [e] The ionic radius used for fluoride is 1.4 Å.

With the exception of the NO_2/NO_2^- couple, the CO_3^{2-}/CO_3^- couple manifests the largest barrier to outer-sphere electron transfer of the reductants considered here. The barrier likely arises from geometry differences between planar carbonate ion and the radical, which is not expected to be planar. However, as is discussed later, a large barrier is expected for this couple because of its small radius (large outer-shell barrier). For SCN^-, previous work can be used only to infer a lower limit of 2×10^2 for the self-exchange.[46] The present study suggests a much greater value, perhaps as great as 1×10^7 M^{-1} s^{-1}. Our result for the $OH^•/OH^-$ couple, 300 M^{-1} s^{-1}, is similar to the values estimated by Schwarz from reactions of $OH^•$ radical with a number of transition-metal complexes.[53] The $OH^•/OH^-$ couple is intermediate between the CO_3^{2-}/CO_3^- and $X^•/X^-$ (X, halogen) couples in its self-exchange rate, qualitatively consistent with an outer-shell barrier dominated process, as is discussed later in more detail.

Although Stanbury[13] has given +1.36 V vs NHE for the HCO_2/HCO_2^- couple, the value +2.0 V inferred by Billing et al.[6] seems more consistent with values for other carboxylates and with other observations and is used here. Arguments have also been given for an even more positive value (≥2.4 V).[15] With $*UO_2F_4^{2-}$, HCO_2^- quenches about 7 times more rapidly than chloride ion; with $*Os^{VI}(tmc)O_2$, the formate ion quenching is about 4 times faster than chloride quenching. With triplet quinones the two anions quench comparably and the formate quenching exhibits no isotope (H–C/D–C) effect, but with aromatic ketones, formate quenching is relatively more rapid and an isotope effect is observed.[15] The latter observations suggest that, for formate-ion oxidations, both outer-sphere electron-transfer and hydrogen-atom-transfer processes may be operative, depending on the nature of the oxidizing agent. The oxygen atoms in the UO_2 and OsO_2 species are potential hydrogen-atom acceptors and there is precedent for H-atom or hydride ion transfer to oxometal complexes. However, there is no indication that such pathways are significant in either the $*UO_2F_4^{2-}$ or $*Os^{VI}(tmc)O_2$ systems.

Outer-Shell Barriers for the Anionic Quenchers. For the halide ion/halogen atom couples the self-exchange rate order I > Br > Cl might have been anticipated on the basis of λ_{out}. (The ionic radii decrease in this order.) On the other hand, the electronic coupling element might be expected to decrease as the halide size increases and the two factors may cancel one another. Another approach to evaluating the intrinsic barriers to electron transfer between cationic metal complexes and halides and other anionic redox reagents is to study the spectroscopic properties of their ion pairs. In Table IV, values of E_{op} reported[54] for halide-to-metal charge-transfer bands of halide–hexaammineruthenium(III) ion pairs are compared with calculated values. The λ_{out} values were

(53) Schwarz, H. A. Unpublished results, 1992.
(54) Waysbort, D.; Evenor, M.; Navon, G. *Inorg. Chem.* **1975**, *14*, 514–519.

obtained from the two-sphere model (eq 4, for water), with

$$\lambda_{out} = 7.85\left(\frac{1}{2a_1} + \frac{1}{2a_2} - \frac{1}{a_1 + a_2}\right) \text{eV} \qquad (4)$$

$a(Ru(NH_3)_6^{3+}) = 3.3$ Å and $a(X^-)$ as given in Tables II and III. Calculations for X = F are included to illustrate the effects of small radius on λ_{out}. (Note that ellipsoidal models for the outer-shell barrier have also been considered.[55]) The $\Delta E°$ values were calculated from the differences between $E°(X^{\bullet}/X^-)$ and $E°(Ru(NH_3)_6^{3+/2+}) = +0.05$ V vs NHE.[56] If the small, constant contribution from $0.5\lambda_{in}(Ru(NH_3)_6^{3+/2+}) = 0.08$ eV[37] and a comparably small contribution to the driving force from w_{12} for the ion-pair formation are neglected, it is evident that the energies of the charge-transfer band maxima are in very good agreement with those predicted by a simple model in which λ is dominated by λ_{out} from eq 4.

The success of the two-sphere model in the present application leads us to use eq 4 to calculate λ_{out} for the $X^{\bullet}/X^-$ couples in water.[57] The results, also listed in Table IV, may be used to set lower limits on the self-exchange rates for the $X^{\bullet}/X^-$ couples in water, neglecting λ_{in}, and assuming that the self exchange is outer-sphere and adiabatic ($\kappa_{el} \sim 1$), but still in the weak interaction limit, eq 5[52] is used. Values obtained from eq 5, with $K_A\kappa_{el}\nu_n =$

$$\Delta G^* = \lambda/4 \qquad (5a)$$

$$k_{el} = K_A\kappa_{el}\nu_n \exp(-\Delta G^*/RT) \qquad (5b)$$

10^{11} M^{-1} s^{-1}, are listed in the last row of Table IV and range from 1×10^{-1} M^{-1} s^{-1} for $F^{\bullet}/F^-$ to 2×10^3 M^{-1} s^{-1} for $I^{\bullet}/I^-$. (Note that the $F^{\bullet}/F^-$ couple provides a good model for the $OH^{\bullet}/OH^-$ couple.) These values are orders of magnitude smaller than the k_{11} values implicated by the cross-reaction data.

The cross relation for the intrinsic barrier to outer-sphere electron transfer is

$$\lambda_{12} = \frac{(\lambda_{11} + \lambda_{22})}{2} \qquad (6)$$

When contributions from λ_{in} are neglected and it is assumed that the oxidized and reduced forms of each couple have the same radius (a_{11} and a_{22} for couple 1 and couple 2, respectively), direct application of eq 4 to the cross reaction yields eq 7, which reduces

$$\lambda_{12} = \frac{\lambda_{11} + \lambda_{22}}{2} + \frac{7.85(a_{11} - a_{22})^2}{4a_{11}a_{22}(a_{11} + a_{22})} \text{eV} \qquad (7)$$

to eq 6 when $a_{11} = a_{22}$. For reactions involving only metal complexes, the situation $a_{11} \sim a_{22}$ is common. However, for the reactions that have been used to probe the outer-sphere reactivity of the halides and other anions considered here, this condition breaks down, the radius of the metal complex generally being much greater than that of the anionic reactant. This breakdown is predicted to yield smaller rate constants for cross reactions of reactants for which a_{11}/a_{22} is very different from unity than would be predicted from the simple cross relation. (In the limit, $a_{11} \ll a_{22}$, the second term in eq 7 goes to $7.85/(4a_{11})$.) Thus when k_{11} is evaluated from eq 3 using known values of K_{12} and k_{22} (the self-exchange rate of the metal–complex couple), the apparent k_{11} value should be even smaller than the calculated value for the $X^{\bullet}/X^-$ exchange given in Table IV.[58] This is illustrated in Figure 7 in which the calculated values for the $X^{\bullet}/X^-$ exchanges (Table IV) and those that would be obtained from analysis of hypothetical cross-reaction data (eq 7) for $a_{22} = 3.3$ Å ($Ru(NH_3)_6$ or $OsO_2(tmc)$) and $a_{22} = 6.8$ Å ($M(bpy)_3$) reactants are plotted against the ionic radius of the anionic reductant.

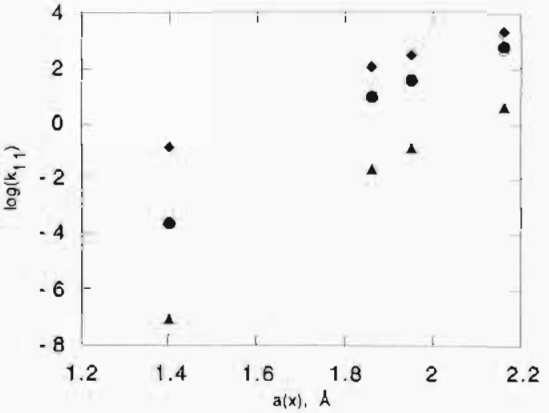

Figure 7. Comparison of calculated values for the (diamonds) $X^{\bullet}/X^-$ exchanges (Table IV) with those obtained from analysis of hypothetical cross reaction data for (circles) $a_{22} = 3.3$ Å ($Ru(NH_3)_6$ or $OsO_2(tmc)$) and (triangles) $a_{22} = 6.8$ Å ($M(bpy)_3$) reactants plotted against the ionic radii for fluoride, chloride, bromide, and iodide.

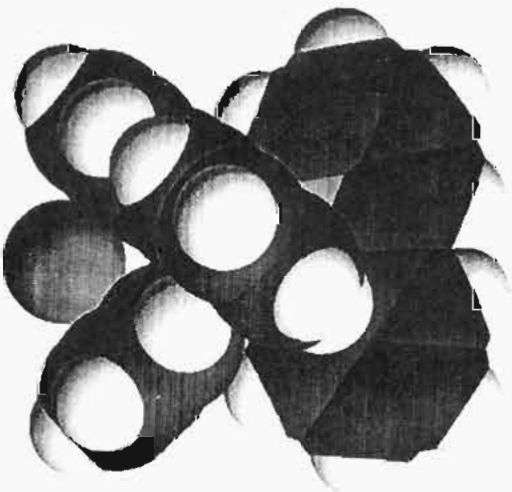

Figure 8. Illustration of an $M(bpy)_3^{3+}/X^-$ ion-pair structure in which the anion rests within one of the six clefts. The case shown is $Ru(bpy)_3^{3+}/F^-$ with the F^- radius set to 1.4 Å. The model was generated from an augmented MM2 force-field molecular-mechanics energy minimization carried out with a Tektronix CACHE molecular graphics software.

The factors considered so far would lead to the expectation that self-exchange rates estimated from cross-reaction data for the halides, etc. should give estimates *lower* than those in Table IV. Instead, the opposite is found. Depending upon the structure of the reaction partner, specific interactions may operate that lead to a great reduction in λ_{out}. For example, for $M(bpy)_3^{3+}/X^-$ reactions, the electron transfer could proceed via "cleft" ion pairs (see Figure 8). The two-sphere model (eq 4) is not applicable for such an arrangement in which r (the M–X center to center

(55) Cannon, R. D. *Chem. Phys. Lett.* **1977**, *49*, 299–304.
(56) Lim, H. S.; Barclay, D. J.; Anson, F. C. *Inorg. Chem.* **1972**, *11*, 1460–1466.
(57) An alternative approach to the evaluation of the barriers for these couples, which is based, in part, on the photoelectron emission techniques and analysis developed by Delahay (Delahay, P.; Dziedzic, A. *Chem. Phys. Lett.* **1986**, *128*, 372–376 and references therein), has recently been described by Loeff et al. (Loeff, I.; Treinin, A.; Linschitz, H. *J. Phys. Chem.* **1992**, *96*, 5264–5272.) Note that the reorganization energies for photoionization, $X^- \rightarrow X^{\bullet} + e_{vac}^-$, and self exchange, $X^- + X^{\bullet} \rightarrow X^{\bullet} + X^-$, will be similar, to the extent that λ_{out} is predominant and that $a_1 = a_2$ (eq 4). In this context, it is of interest that the λ_{out} values for the $X^-/X^{\bullet}$ self-exchange reactions presented in Table IV are typically 0.3 eV larger than the "single ion" values determined by photoelectron spectroscopy.
(58) The failure of the cross-relation for reactions of couples with very different sizes has also been noted by others. See: Awad, H. H.; Stanbury, D. M. *J. Am. Chem. Soc.* **1993**, *115*, 3636–3642. Merenyi, G.; Lind, J.; Jonsson, M. *J. Am. Chem. Soc.* **1993**, *115*, 4945–4946 and references therein.

distance) $\ll a_1 + a_2$. (For $M(bpy)_3^{3+}/X^-$, the following values are found (X, r, $a_1 + a_2$): I, 5.5, 8.9; Br, 5.27, 8.75; Cl, 5.1, 8.61; F, 4.5, 8.2.) "Outer-sphere" electron transfer via "cleft" ion pairs should be subject to only a very small λ_{out}. In addition, since the anion is effectively sitting on the lobe of one of the πd orbitals, the electronic interactions between electron donor and acceptor may be so great that the electron-transfer process is not in the weak-interaction limit.

However, given that all of the cross reactions studied so far for the halides (and for thiocyanate in the present work) lead to self-exchange estimates so much greater than those predicted from λ_{out} calculations, it does not seem useful to invoke special interactions as a universal rationalization. Instead, it seems most reasonable to acknowledge that redox reactions of the halides (and thiocyanate) with normally outer-sphere reaction partners involve strong electronic interaction. If this is the case, the k_{11} value should depend on the reaction partner to some degree. While such a dependence on reaction partner has been found for O_2/O_2^- reactions[59] and may be discernible in the iodide oxidation data (Table III), it remains to be seen for the other halides and thiocyanate, there being few data at present. Finally, it is worth emphasizing that, unlike the halides and thiocyanate, significant barriers to outer-sphere electron transfer are exhibited by azide, nitrite, formate, carbonate, and hydroxide.

Concluding Remarks. The present study provides preliminary characterization of the $^*Os^{VI}O_2(tmc)^{2+}/Os^{V}O_2(tmc)^+$ couple in aqueous media. The behavior observed with the aqua-ion quenchers is in reasonable agreement with $^*E^\circ = +2.26$ V and a self-exchange rate constant of 1×10^5 M^{-1} s^{-1}. Use of the highly oxidizing excited state has provided an opportunity for characterization of the self-exchange rates of a number of couples involving small anions. The first estimates are presented for the CO_3^{2-}/CO_3^- (0.4 M^{-1} s^{-1}), $OH^\bullet/OH^-$ (300 M^{-1} s^{-1}), and HCO_2/HCO_2^- (300 M^{-1} s^{-1}) couples. Self-exchange rates for the $X^\bullet/X^-$ halogen couples, calculated assuming that only the outer-shell barrier contributes to the intrinsic barrier to outer-sphere electron transfer and that a two-sphere dielectric continuum model is applicable, are orders of magnitude smaller than the self-exchange rates inferred from the quenching data and literature data. Thus it seems likely that redox reactions of the halides (and thiocyanate) with normally outer-sphere reaction partners involve strong electronic interaction. However, unlike the halides and thiocyanate, azide, nitrite, formate, carbonate, and hydroxide do exhibit significant barriers to outer-sphere electron transfer.

Acknowledgment. We thank Dr. B. Brunschwig for undertaking transient absorption measurements, Dr. E. Fujita for helpful comments on the NMR work, and Drs. H. A. Schwarz, D. M. Stanbury, H. Linschitz, and R. Billing for helpful discussions on the anion couples. The research was carried out at Brookhaven National Laboratory under Contract DE-AC02-76CH00016 with the U.S. Department of Energy and supported by its Division of Chemical Sciences, Office of Basic Energy Sciences.

(59) McDowell, M. S.; Espenson, J. H.; Bakac, A. *Inorg. Chem.* **1984**, *23*, 2232–2236.